Network analysis in Gamma Knife capsulotomy for intractable obsessive-compulsive disorder

Tim A.M. Bouwens van der Vlis [a,*], Yavuz Samanci [b], Linda Ackermans [a,c], Koen R.J. Schruers [c,d], Y. Temel [a,c], Albert F.G. Leentjens [c,d], Alp Dincer [e], Selçuk Peker [b]

[a] Department of Neurosurgery, Maastricht University Medical Centre, Maastricht, the Netherlands
[b] Department of Neurosurgery, School of Medicine, Koç University, Istanbul, Turkey
[c] School of Mental Health and Neuroscience, Maastricht University, Maastricht, the Netherlands
[d] Department of Psychiatry and Psychology, Maastricht University Medical Center, Maastricht, the Netherlands
[e] Department of Radiology, Acıbadem Mehmet Ali Aydınlar University, Istanbul, Turkey

A B S T R A C T

Introduction: Gamma-knife Ventral Capsulotomy (GVC) has been suggested as an efficacious treatment for a subset of patients with treatment refractory obsessive compulsive disorder (OCD).

Research question: The goal of this study was to investigate neural correlates of GVC and investigate the predictive value of white matter tracts that are known to be associated with clinical outcome to Deep Brain Stimulation (DBS).

Material and methods: MR images of 8 treatment-refractory OCD patients with a minimum follow-up of 3-years who underwent GVC were used to correlate lesion characteristics with symptom improvement. This exploratory study investigated relations between differences in cortical grey matter structure and subcortical structures before and after GVC for responding and non-responding patients (n = 6). Normative diffusion MRI- based tractography was used to determine networks associated with successful lesions.

Results: The mean total Y-BOCS reduction was 19.6 after three years, resulting in a response rate of 63%.The strongest correlation with symptom improvement was found for a decrease of the left ventral diencephalon volume (r = −0.83, p = 0.039). Discriminative tractography suggest streamlines connecting the prefrontal cortex with the subthalamic nucleus to be associated with clinical response. However, results could not be validated either implicating interpatient anatomical variability or reflecting the relative small sample size as a limitation.

Discussion/Conclusion: Taken together, the present study highlights the efficacy of GVC in patients with treatment-refractory OCD. Our results are suggestive of GVC treatment efficacy being mediated by the involvement of a subpart of the ALIC connecting the PFC and the STN.

1. Introduction

Obsessive-compulsive disorder (OCD) is characterized by recurrent, unwanted, and disturbing obsessions (thoughts, urges or images) and/or repetitive behaviors/mental acts (compulsions) aimed at reducing or preventing anxiety or distress. OCD has an estimated lifetime prevalence of 1.6% and is associated with a higher risk of suicide, an increased risk of metabolic and cardiovascular disorders and increased rates of long-term labor-market marginalization (De La Cruz et al., 2017; Isomura et al., 2018; P é rez-Vigil et al., 2019; Kessler et al., 2005). Most patients will experience some symptom relief after receiving cognitive behavioral therapy (CBT) and selective serotonin reuptake inhibitors (SSRIs) either alone or in combination (Hirschtritt et al., 2017). However, an estimated proportion of 40–60% responds insufficiently to treatment, prompting

the investigation of alternative treatment augmentation strategies, i.e. switching to a different SSRI or clomipramine, addition of neuroleptic agents and ultimately, neuromodulation therapies or ablative surgery (Hirschtritt et al., 2017).

Neurosurgical techniques, focused on lesioning or modulating components of the neural circuitry implicated in OCD, have been used for decades in the treatment of adults with severe, treatment-refractory symptoms. Neurobiological models posit that dysfunction of corticostriatal-basal ganglia-cortical circuits (CBGCs) connecting orbitofrontal cortex, anterior cingulate, basal ganglia, and thalamus underlie OCD pathophysiology as evidenced in neuroimaging studies (Whiteside et al., 2004; Burgui è re et al., 2015). Four main ablative procedures have emerged for treatment-refractory OCD: anterior capsulotomy, anterior cingulotomy, subcaudate tractotomy and limbic leucotomy (a

combination of anterior cingulotomy and subcaudate tractotomy) (Lai et al., 2020; Sinha et al., 2015). Among these ablative procedures, anterior capsulotomy has been associated with the highest response rate (Lai et al., 2020). Contemporary techniques for anterior capsulotomy include Gamma Knife radiosurgery (GKRS), magnetic resonance-guided ultrasonography (MRgFUS and laser interstitial thermal therapy (LITT) (Lai et al., 2020; Satzer et al., 2021; Kim et al., 2018). Deep Brain Stimulation (DBS), a nonablative and adjustable procedure was introduced in 1999 as an alternative treatment to ablative surgery for treatment-refractory OCD (Nuttin et al., 1999). The effectiveness of DBS, aimed at different target structures for OCD, has subsequently been established by several placebo controlled randomized controlled trials (Mosley et al., 2021; Luyten et al., 2016; Mallet et al., 2008; Denys et al., 2010). A recent meta-analysis showed an equal efficacy of ablative surgery compared to DBS (Hageman et al., 2021). However, for DBS of the nucleus accumbens (NA) a higher rate of mild and transient impulsivity has been reported (Hageman et al., 2021). A significant body of literature demonstrates that electrical stimulation is able to suppress abnormal activity in frontolimbic circuits associated with OCD, thereby associating specific white matter tracts with clinical response, Fig. 1 (Figee et al., 2013; Fridgeirsson et al., 2020; Treu et al., 2021; Baldermann et al., 2021). Similar functional and anatomical analyses for Gamma Knife anterior capsulotomy remain scarce (Satzer et al., 2021).

This study aims to contribute to the anatomical understanding of anterior capsulotomy by morphometric analyses and incorporating recent connectomic findings in DBS-OCD literature into imaging data of 8 treatment-refractory OCD patients treated with GKRS.

2. Methods

2.1. Patients/Gamma Ventral Capsulotomy procedure

In this retrospective cohort, 8 patients were selected for Gamma Knife Ventral Capsulotomy (GVC) between the period of 2011–2016 according to the inclusion criteria as previously described (Peker et al., 2020). These patients were from a previously described cohort of treatment refractory OCD patient treated with GVC and selected based on the availability of post-GVC MRI data (Peker et al., 2020). These criteria included the diagnosis of severe OCD on the basis of DSM-IV, with a Yale-Brown Obsessive-Compulsive Scale (Y-BOCS) score of at least 25. This level of impairment should have persisted for a minimum of 5 years, despite adequate trials or intolerance to two selective serotonin reuptake inhibitors and clomipramine, augmentation strategies (i.e., antipsychotic medications), and CBT. Patients with a reduction in Y-BOCS scores of 35% or more were considered responders.

GKRS was performed using Leksell Gamma Knife® model 4C (2009–2012) or Perfexion™ (2012–2016). A Leksell stereotactic frame (Elekta Instrument, Stockholm, Sweden) was mounted on the skull under local anesthesia, and a peri-operative contrast enhanced MRI-scan of the head with frame was acquired. Treatment plans were performed using the GammaPlan Software (Elekta Instruments, Stockholm, Sweden). The bilateral target was the most ventral margin in the center of the ALIC. The targets were irradiated by a maximum dose of 140–150 Gy with 1 or 2 shots using 4-mm collimators (Peker et al., 2020). For a more detailed description of GVC procedures, we refer to earlier papers (Peker et al., 2020; Akyoldas et al., 2021).

2.2. Imaging, GVC-lesion segmentation and normalization

All subjects had a 3-T MRI 1 year after GVC (Siemens, Erlangen, Germany). The sequence used was a 3D T1 (voxel size $1 \times 1 \times 1$mm) with gadolinium. GVC volumes were segmented on T1 sequences in ITK-SNAP V.3.8.0 (itksnap.org) as the contrast-enhancing volume including the hypointense center (Yushkevich et al., 2006). Pre-GVC MR-images were normalized into ICBM 2009b Non-linear Asymmetric ("MNI") template space using the SyN approach implemented in Advances Normalization Tools (ANTs), with an additional subcortical refinement stage as provided in the Lead-DBS pipeline (Avants et al., 2014; Horn et al., 2019; Treu et al., 2020). GVC volumes were then normalized into ICBM 2009b Non-linear Asymmetric ("MNI") template space using SPM12 (fil.i-on.ucl.ac.uk/spm) as provided in Lead-DBS. In the absence of Pre-GVC MR-images (n = 2), GVC volumes were normalized into MNI template space as implemented in LESYMAP, a package available in R (Pustina et al., 2018). Ablation volumes were averaged to create heat maps and subsequently binarized for normative tractography analysis (Satzer et al., 2021; Jenkinson et al., 2012). Heatmaps were visualized in FSLeyes 5.0.10 (McCarthy, 2021).

2.3. Morphometry

All available pre-post GVC MR-images (n = 6) were processed using Freesurfer image analyses suite version 7.2, which automatically reconstructs a three-dimensional model of the cortical surface for cortical thickness measurement and provides a mean thickness and volume within automatically defined cortical parcellations and subcortical segmentations in each hemisphere and freely available for download online (http://surfer.nmr.mgh.harvard.edu/). The technical details of these procedures are described in prior publications (Fischl et al., 2004; Fischl and Dale, 2000; Dale et al., 1999). Minor adjustments to the automated segmentation and parcellation routines were made when necessary (e.g. adding control points to facilitate grey/white matter classification), but no major alterations were necessary. The left and right hemispheres were registered to the fsaverage atlas (common surface space) templates included in Free-Surfer, and smoothed with a Gaussian kernel of FWHM 10 mm.
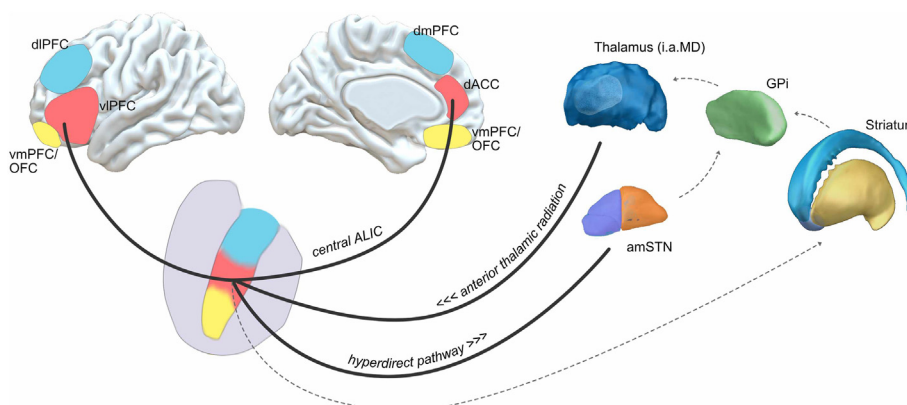

Fig. 1. Reprinted from Baldermann *et al*, with permission from Elsevier and the leading author (Baldermann et al., 2021). A proposed mechanism of action for ALIC DBS, hypothesized to be involved in GVC. Displayed are areas implicated in the pathophysiology of obsessive-compulsive disorder (upper right) and their representation within the anterior limb of the internal capsule (ALIC) (bottom left). The right panel schematically illustrates connections with the basal ganglia. The central ALIC serves as a hub for various pathways associated with OCD; the vlPFC to dACC and STN pathways as well as the thalamus to vlPFC pathway. Abbreviations; dACC: dorsal anterior cingulate cortex; vlPFC ventrolateral prefrontal cortex; amSTN: anteromedial subthalamic nucleus; MD thalamus: medial dorsal nucleus of the thalamus; vmPFC ventro-medial PFC; OFC: orbitofrontal cortex; dmPFC: dorsomedial prefrontal cortex; GPi: globus pallidus internus.

Separate General Linear Models (GLMs) were constructed to analyze the effect of GVC on cortical volume and thickness (GMV, GMT; pre-vs. post-GVC) and correlation with OCD symptom reduction. All vertex-wise results were thresholded at an individual vertex level of $p <$ 0.001, and cluster extent thresholds corrected for multiple comparisons with a 5% (FDR) were calculated through Monte Carlo simulations of white noise on the cortical surface. The model included Y-BOCS reduction and patient age. We did not include Total Intracranial Volume (TIV) in the model as a covariate in the GLMs, as we were specifically concerned with modelling correlations with individual differences in GMV and GMT. For subcortical structure analyses, we included 10 subcortical structures for each hemisphere. The subcortical volumes were not corrected for TIV. Individual Y-BOCS reduction was correlated with the difference of pre- and post-GVC subcortical structure volumes.

2.4. Normative tractography

In order to identify discriminating fiber bundles associated with clinical response to GVC, we adapted the methodology of Li et al. (Baldermann et al., 2021; van der Vlis et al., 2021; Li et al., 2020a) Accordingly, based on a normative connectome, individual fibers were assigned a 'Fiber T-score' by correlating the fiber tract's connectivity to GVC volumes across patients with clinical outcome (Irmen et al., 2020; Van Essen et al., 2013). Validation of the tracts was sought by performing a k-fold cross prediction. Second, connectivity estimates were calculated between the averaged (non-) responder ablation volumes and cortical parcels of the PFC, as provided in Lead DBS. MNI cortical parcels of the PFC were generated by combining Brodmann areas 8, 9, 10, 46 (dorsolateral PFC); 44, 45, 47 (ventrolateral PFC); and 12, 25, 32, 33, 34 (ventromedial PFC) as provided in the Brodmann Atlas of the WFU PickAtlas v2.4 in SPM12 (Maldjian et al., 2003).

2.5. Gamma Ventral Capsulotomy vs. Deep brain stimulation for intractable obsessive-compulsive disorder

To provide for a direct anatomical comparison between GVC lesion volumes and DBS Volume of Tissue Activation (VTA), we combined data of 8 previously described OCD patients receiving ventral capsule/ventral striatum VC/VS stimulation (van der Vlis et al., 2021). The Euclidean distance between 'hottest' voxel of the averaged GVC volumes and VTAs was calculated using MATLAB (R2020a, Mathworks, Natick, Massachusetts). Recent connectomic findings in DBS for OCD, have identified a connectivity profile positively associated with clinical outcome (Baldermann et al., 2021). Specifically, streamlines connecting dorsal anterior cinculate cortex (dACC), the lateral and medial prefrontal cortex with the anteromedial STN and medial dorsal nucleus of the thalamus were associated with successful DBS (Baldermann et al., 2021). This tractographic profile was made publicly and available within Lead-DBS (Horn et al., 2019). In order to identify the positive predictive value of these 'DBS' tracts in GVC we adapted the sum-score methodology as described in Li et al., by calculating how many of the DBS associated fibers passed through the patients' GVC volume. Then, for each patient a fiber score was calculated: a sum-score weighted by the t-value of each tract passing through each GVC. As GVC volumes were asymmetrical, we analyzed the left and right hemispheres separately.

2.6. Statistical analyses

Clinical outcome variables, fiber count estimates and GVC volumes were compared between non-responders and responders using Mann-Whitney U test. GVC-atlas intersection volumes and (sub)-cortical structure volumes were correlated with treatment outcome using Spearman's correlation and Bonferroni corrected. The Kolmogorov-Smirnov was used to test for normality. P-values<0.05 were considered statistically significant. Unless otherwise indicated, results will be displayed as a mean ± SD. All statistical analyses were performed using IBM SPSS Statistics, version 20 (IBM Corp., Armonk, N.Y., USA).

3. Results

3.1. Patient characteristics

We included 8 treatment-refractory OCD patients with a minimum follow-up of 3-years after with GVC. The mean age of the participants was 35 ± 7.5 years. For a detailed disease and treatment history we refer to our previous publication (Peker et al., 2020). The steepest descent in total Y-BOCS scores was observed between 6 months and 1 year −7.1 ± 5.6. Further improvement was observed after one year. At three years follow-up, five patients were considered a responder, while three remained non-responsive, resulting in a response rate of 63%, Fig. 2a. The mean total Y-BOCS reduction was 19.6 after three years, with an equal reduction in YBOCS subscores for obsessions and compulsions. Specified for responders, the mean total YBOCS reduction was 28.8. There were no significant differences in age at surgery, gender or follow-up time at baseline between responders.

3.2. Lesion geometry

The mean time between GVC and post-operative imaging was 229 days [89–370 days]. MNI coordinates of the 'hottest' voxels of the averaged lesions of the responding patients were [−20, 18.5, −1.5] for the left hemisphere and [16, 18.5, −1.5] for the right hemisphere, whereas the 'coldest' voxels for non-responding patients was [−17, 16, −8] vs. (Mallet et al., 2008; Denys et al., 2010), Fig. 3b. The mean total GVC volume (left plus right) was 326.5 ± 112.9 mm³, with non-significant larger GVC volumes in the left hemisphere (193.6 ± 165.7 mm³) when compared to the right hemisphere (112.9 ± 112.9 mm³), Fig. 2c. No differences were observed for lesion volumes of responders vs. non-responders. Improvement in Y-BOCS was not correlated with left ($p = 0.867$) or right ($p = 0.469$) GVC volume. Volumes of the caudate (left $p = 0.529$, right $p = 0.763$), putamen (left $p = 0.545$, right $p = 0.736$), nucleus accumbens (left $p = 0.505$, right $p = 0.823$), and globus pallidus externus (left $p = 0.258$, right $p = 0.555$) ablated were not correlated with total Y-BOCS reduction, Fig. 3a.

3.3. Morphometry

Our whole brain analysis revealed no differences of GMV or GMT in both hemispheres following GVC, or correlations between Y-BOCS reduction and cortical structures. Of the 10 ICV corrected subcortical structures in each hemisphere, a negative correlation was found for the left ventral diencephalon, including hypothalamus with mammillary body, subthalamic, lateral geniculate, medial geniculate and red nuclei, substantia nigra, and surrounding white matter ($r = -0.83$, $p = 0.039$) and the right cerebellum white matter ($r = -0.78$ $p = 0.042$). There were no differences in pre-GVC subcortical volumes between responders and non-responders.

3.4. Connectivity analyses

Fiber T-values to GVC volumes were assigned across patients with clinical outcome as performed in, Baldermann et al. (2019) Tracts were thresholded to be connected to 20% of GVC volumes. Fiber bundles positively associated with the percentage Y-BOCS reduction originate from the PFC of which a subset to the project to subthalamic nucleus (STN), in accordance with identified tracts associated with DBS response for OCD (Li et al., 2020a). Projections traversing through the superior genu of the corpus callosum were negatively associated with GVC response, Fig. 3b However, we were unable to validate the identified tracts in a subsequent prediction analysis using k-fold (K = 2) cross validation ($r = 0.13$, $p = 0.382$). There were no differences in fiber count estimates between (non-) responder GVC volumes and the dlPFC, vlPFC or the vmPFC, Fig. 3c.
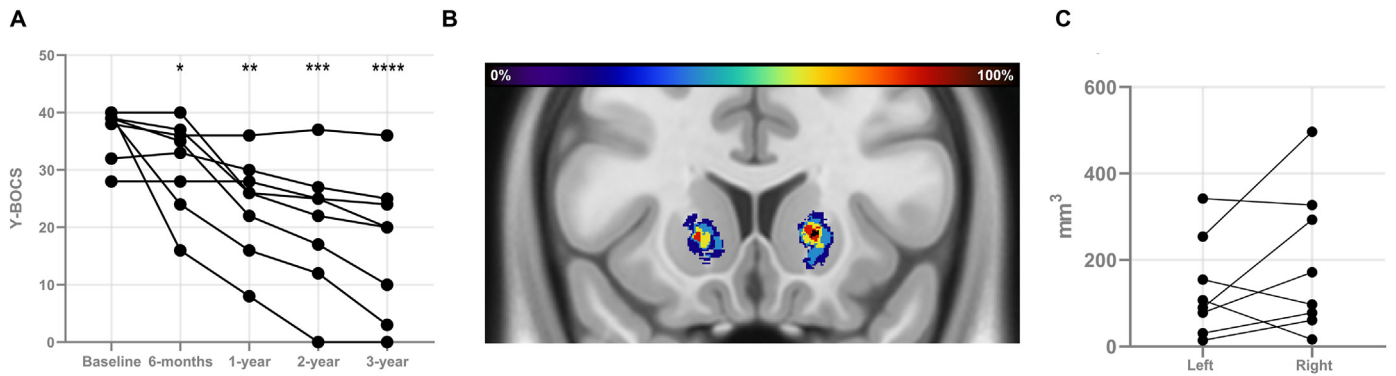
Fig. 2. A. Individual Yale-Brown Obsessive Compulsive Scale (Y-BOCS) scores for obsessive-compulsive disorder (OCD) patients treated with GVC (A) (*p = 0.11; **p = 0.014; ***p = 0.011; ****p = 0.007). B. Heatmap representing the averaged GVC volumes in ICBM 2009b Non-linear Asymmetric MNI template C. Individual GVC volumes for the left and right hemisphere (C). (For interpretation of the references to colour in this figure legend, the reader is referred to the Web version of this article.)
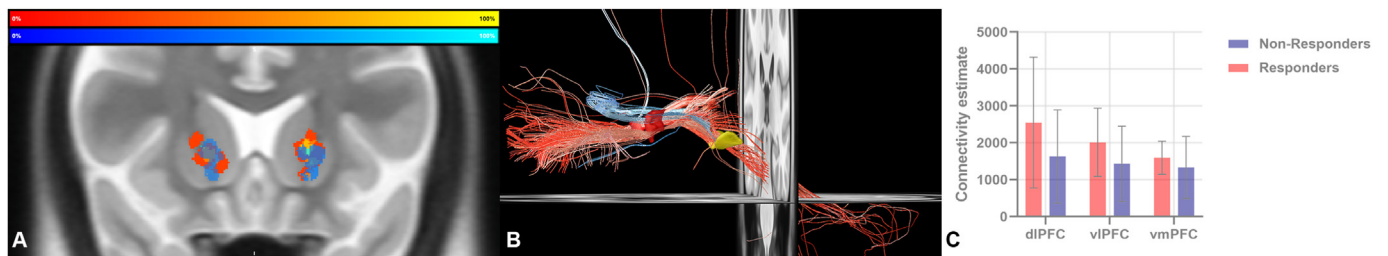

Fig. 3. A. Heatmap representing the averaged GVC volumes for responders (red-yellow) and non-responders (blue-light blue) in ICBM 2009b Non-linear Asymmetric MNI template. B. Positive (A) and Negative (B) predicting fibers associated with clinical improvement are shown in red and blue. Dark red: concatenated GVC volumes. Yellow: Subthalamic nucleus. **C.** Connectivity estimates between GVC volumes of (non-) responders and the dorsolateral, ventrolateral and ventromedial prefrontal cortex. (For interpretation of the references to colour in this figure legend, the reader is referred to the Web version of this article.)

3.5. Gamma Ventral Capsulotomy vs. Deep brain stimulation for intractable obsessive-compulsive disorder

In comparison to the volume of tissue activation of DBS, GVC volumes were located more anterolaterally, with an Euclidean distance of 16.5 and 16.8 between the MNI coordinates of the 'hottest voxels' of averaged VTAs [−8.14, 2.13, −3.91; −17.5, 15.5, 0] and GVC volumes [9.99, 3.23, −3.03; 16; 18.5; −1.5], Fig. 4a. In 4/8 patients GVC ablated bilaterally (a part of) a subtract of the anterior limb of the internal capsule, connecting the prefrontal cortex to the subthalamic nucleus and the mediodorsal nucleus (MD) of the thalamus positively associated with YBOCS reduction, whereas in two patients unilateral involvement of this tract was found (Baldermann et al., 2019). In one patient, GVC volumes did not affect this tract Fig. 4b. We were unable to replicate the association with the previously implicated tracts with clinical response, ($p_{one-tailed}$ = 0.786, Fig. 4c).

4. Discussion

Our analysis of a subset of patients from a previously described cohort of treatment refractory OCD patient treated with GVC supports its clinical effectiveness. The responder rate of 63% and a mean Y-BOCS reduction of 51% after three years of follow up compares favorably with previous reports of GVC for OCD (Hageman et al., 2021). The current study was unable to support claims that ablative surgery potentially provides immediate relief of OCD symptoms as the maximum response rate was reached after two years of follow-up (Zhan et al., 2014).

Only a few studies report on lesion volume after ablative surgery for OCD with respect to outcome, where results are contradictory as lesion volume can be positively and negatively associated with outcome (Satzer et al., 2021; R ü ck et al., 2008; Lippitz et al., 1999). There is a noteworthy degree of both intra- and inter-modality variability of lesion
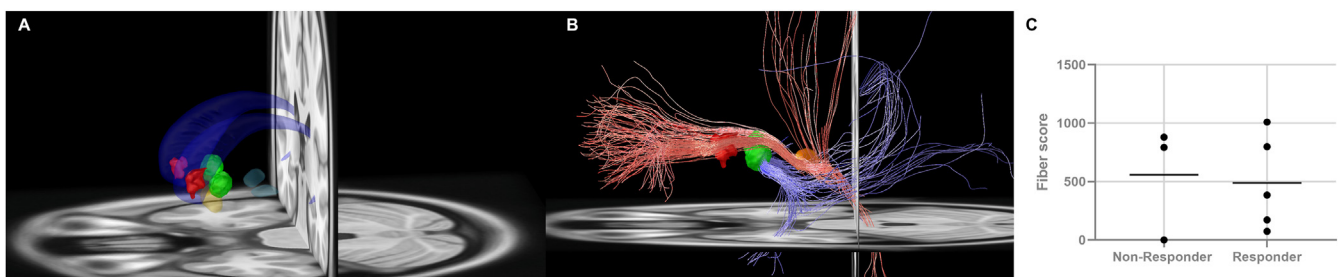

Fig. 4. A. Location of GVC volumes (red) in relation to concatenated DBS VTAs (green), caudate nucleus (dark blue), nucleus accumbens (yellow) and subthalamic nucleus (light blue) B. Positive (A) and Negative (B) predicting fibers previously associated with clinical improvement to DBS are shown in red and blue. **C.** Association between previously implicated white matter fibers and clinical response to OCD DBS. (For interpretation of the references to colour in this figure legend, the reader is referred to the Web version of this article.)

volumes with a mean total lesion volume following LITT 2400 ± 600 mm^3 versus GVC 1737 ± 924 mm^3 and lesion volume after MRgFUS lesioning of 362 ± 290 mm^3. Further, hemispherical lesion asymmetry is a common finding following bilateral GVC, as was observed in this case series (Rück et al., 2008; Lippitz et al., 1999). Recent advances highlight the importance of the anatomical location of the lesion (Satzer et al., 2021; Germann et al., 2021). Probabilistic voxel wise efficacy maps of magnetic resonance-guided focused ultrasound MRgFUS treated OCD patients show the region associated with the highest symptom improvement located in the anterodorsal aspect of the ALIC, with an identified region associated with clinical efficacy centred around x = (−) 15.5 (±1 mm), y = 10 (±2 mm), z = 4 (±1 m). When compared, GVC lesions associated with symptom improvement in this study were also located in the anterodorsal aspect of the ALIC. However, we were unable to identify an overall difference in Euclidean distance between the 'hottest' voxel of lesions of responders versus non-responders to GVC and the identified MRgFUS sweetspot (Germann et al., 2021).

Different regions of the ALIC carry fibers from different prefrontal regions with a ventral–dorsal, medial–lateral, and anterior–posterior organisational topography (Safadi et al., 2018). Converging evidence from pre-operative DTI and normative connectivity studies identified specific tracts and fibers associated with clinical outcome. Following both ALIC and STN DBS the most clinical effective contacts stimulated thalamocortical ALIC streamlines to the dorsolateral and medial PFC and the rostral anterior cingulate (dACC) (Baldermann et al., 2019; Li et al., 2020b). Furthermore, normative resting-state functional MRI analyses showed that lesion engagement following MRgFUS of the dACC and left dlPFC was correlated with symptom engagement. In our sample, we were not able to replicate the association between ALIC tracts implicated in DBS and clinical response, finding responder and non-responder fiber scores were not different. Further, we were not able to highlight the functional lesional connectivity with the dACC and the dlPFC (data not shown). The inability to replicate both findings could reflect the small sample size as the principal limitation of this study. Using the same methodology our group and others were able to validate and replicate the thalamocortical ALIC streamlines associated with clinical outcome in DBS in relatively small sample sizes (n = 8, n = 10) (van der Vlis et al., 2021; Smith et al., 2021). Implicating that clinical response to OCD-GVC moves beyond a unified connectomic target as response to OCD-GVC was found independent of centroid coordinates and lesion volume in a large cohort of radiofrequency anterior capsulotomy, suggested to be caused by nontrivial intersubject variability of ALIC fiber organization (Lv et al., 2021a; Nanda et al., 2017). Moreover, structural predictors of good clinical response to capsulotomy include a decreased grey matter volume of the right inferior frontal gyrus, fiber integrity of the superior longitudinal fasciculus, and lower connectivity of the dorsal caudate with the dACC and an increased streamline counts of the dlPFC – thalamic tracts (Lv et al., 2021a; Zhang et al., 2021; Yin et al., 2018).

Our analysis revealed a negative correlation of symptom improvement with the subcortical volume of the left ventral diencephalon including the hypothalamus with mammillary body, subthalamic, lateral geniculate, medial geniculate and red nuclei, substantia nigra and surrounding white matter and right cerebellar white matter. A post-hoc analysis revealed no differences of the volumes of the left ventral diencephalon area or the cerebellum pre-surgery, indicating that variability in response is more likely to be a therapeutic effect. Cerebellar volume alterations were previously shown following thermo-capsulotomy, suggested to be secondary to thalamic atrophy (Lv et al., 2021b). The structures involved in the ventral diencephalon are part of frontostriatal networks identified to be functionally restored by DBS or GVC (Figee et al., 2013; Lv et al., 2021b). Taken together, the left ventral diencephalon might contribute to the effects of GVC.

Taken together, the present study highlights the efficacy of GVC in patients with treatment-refractory OCD. We were not able to identify discriminative fiber tracts associated with GVC clinical response, nor predict clinical outcome using previously identified tracts in DBS,

implicating interpatient variability i.e. ALIC fiber organization explanatory for treatment variability. Future research should focus on elucidating neuroanatomical substrates of OCD symptom dimensions and ideally identify the optimal for structural profile relevant to treatment targets for both ablative and invasive neuromodulation for treatment refractory OCD.

Statement of ethics

Funding sources

Author contributions

Data availability statement

Declaration of competing interest

References

Akyoldas, G., Samanci, Y., Tugcu, E.S., Peker, S., 2021 Dec. Gamma Knife radiosurgery for the treatment of central neurocytoma: a single-institution experience of 25 patients. Neurosurg. Rev. 44 (6). https://doi.org/10.1007/S10143-021-01518-0.

Avants, B.B., Tustison, N., Johnson, H., 2014. Advanced Normalization Tools (ANTS) Release 2.x [cited 2021 Nov 24]. Available from: https://brianavants.wordpress.com/2012/04/13/updated-ants-compile-instructions-april-12-2012/.

Baldermann, J.C., Melzer, C., Zapf, A., Kohl, S., Timmermann, L., Tittgemeyer, M., et al., 2019 May. Connectivity profile predictive of effective deep brain stimulation in obsessive-compulsive disorder. Biol. Psychiatr. 85 (9), 735–743.

Baldermann, J.C., Schüller, T., Kohl, S., Voon, V., Li, N., Hollunder, B., et al., 2021 Nov. Connectomic deep brain stimulation for obsessive-compulsive disorder. Biol. Psychiatr. 90 (10), 678–688.

Burguière, E., Monteiro, P., Mallet, L., Feng, G., Graybiel, A.M., 2015 Jan. Striatal circuits, habits, and implications for obsessive-compulsive disorder. Curr. Opin. Neurobiol. 59, 0.

Dale, A.M., Fischl, B., Sereno, M.I., 1999. Cortical surface-based analysis. I. Segmentation and surface reconstruction. Neuroimage 9 (2), 179–194.

De La Cruz, L.F., Rydell, M., Runeson, B., D'Onofrio, B.M., Brander, G., Rück, C., et al., 2017 Nov. Suicide in obsessive-compulsive disorder: a population-based study of 36 788 Swedish patients. Mol. Psychiatr. 22 (11), 1626–1632.

Denys, D., Mantione, M., Figee, M., Van Den Munckhof, P., Koerselman, F., Westenberg, H., et al., 2010. Deep brain stimulation of the nucleus accumbens for treatment-refractory obsessive-compulsive disorder. Arch. Gen. Psychiatry 67 (10), 1061–1068.

Figee, M., Luigjes, J., Smolders, R., Valencia-Alfonso, C.E., Van Wingen, G., De Kwaasteniet, B., et al., 2013 Apr. Deep brain stimulation restores frontostriatal network activity in obsessive-compulsive disorder. Nat. Neurosci. 16 (4), 386–387.

Fischl, B., Dale, A.M., 2000 Sep. Measuring the thickness of the human cerebral cortex from magnetic resonance images. Proc. Natl. Acad. Sci. U. S. A. 97 (20), 11050–11055.

Fischl, B., Van Der Kouwe, A., Destrieux, C., Halgren, E., Ségonne, F., Salat, D.H., et al., 2004 Jan. Automatically parcellating the human cerebral cortex. Cerebr. Cortex 14 (1), 11–22.

Fridgeirsson, E.A., Figee, M., Luigjes, J., van den Munckhof, P., Richard Schuurman, P., van Wingen, G., et al., 2020 May. Deep brain stimulation modulates directional limbic connectivity in obsessive-compulsive disorder. Brain 143 (5), 1603–1612.

Germann, J., B Elias, G.J., Neudorfer, C., Boutet, A., Chow, C.T., Y Wong, E.H., et al., 2021 Dec. Potential optimization of focused capsulotomy for obsessive compulsive disorder. Brain 144 (11), 3529–3540.

Hageman, S.B., van Rooijen, G., Bergfeld, I.O., Schirmbeck, F., de Koning, P., Schuurman, P.R., et al., 2021 Apr. Deep brain stimulation versus ablative surgery for treatment-refractory obsessive-compulsive disorder: a meta-analysis. Acta Psychiatr. Scand. 143 (4), 307–318.

Hirschtritt, M.E., Bloch, M.H., Mathews, C.A., 2017 Apr. Obsessive-compulsive disorder: advances in diagnosis and treatment. JAMA 317 (13), 1358–1367.

Horn, A., Li, N., Dembek, T.A., Kappel, A., Boulay, C., Ewert, S., et al., 2019 Jan. Lead-DBS v2: towards a comprehensive pipeline for deep brain stimulation imaging. Neuroimage 184, 293–316.

Irmen, F., Horn, A., Mosley, P., Perry, A., Petry-Schmelzer, J.N., Dafsari, H.S., et al., 2020 Jun. Left prefrontal connectivity links subthalamic stimulation with depressive symptoms. Ann. Neurol. 87 (6), 962–975.

Isomura, K., Brander, G., Chang, Z., Kuja-Halkola, R., Rück, C., Hellner, C., et al., 2018 Sep. Metabolic and cardiovascular complications in obsessive-compulsive disorder: a total population, sibling comparison study with long-term follow-up. Biol. Psychiatr. 84 (5), 324–331.

Jenkinson, M., Beckmann, C.F., Behrens, T.E.J., Woolrich, M.W., Smith, S.M., 2012 Aug. FSL. Neuroimage 62 (2), 782–790.

Kessler, R.C., Berglund, P., Demler, O., Jin, R., Merikangas, K.R., Walters, E.E., 2005 Jun. Lifetime prevalence and age-of-onset distributions of DSM-IV disorders in the national comorbidity survey replication. Arch. Gen. Psychiatr. 62 (6), 593–602.

Kim, S.J., Roh, D., Jung, H.H., Chang, W.S., Kim, C.H., Chang, J.W., 2018 Sep. A study of novel bilateral thermal capsulotomy with focused ultrasound for treatment-refractory obsessive–compulsive disorder: 2-year follow-up. J. Psychiatry Neurosci. 43 (5), 327.

Lai, Y., Wang, T., Zhang, C., Lin, G., Voon, V., Chang, J., et al., 2020 Sep. Effectiveness and safety of neuroablation for severe and treatment-resistant obsessive-compulsive disorder: a systematic review and meta-analysis. J. Psychiatry Neurosci. 45 (5), 356–369.

Li, N., Baldermann, J.C., Kibleur, A., Treu, S., Akram, H., Elias, G.J.B., et al., 2020 Dec. A unified connectomic target for deep brain stimulation in obsessive-compulsive disorder. Nat. Commun. 11 (1). https://doi.org/10.1038/s41467-020-16734-3.

Li, N., Baldermann, J.C., Kibleur, A., Treu, S., Akram, H., Elias, G.J.B., et al., 2020 Jul. A unified connectomic target for deep brain stimulation in obsessive-compulsive disorder. Nat. Commun. 11 (1), 1–12.

Lippitz, B.E., Mindus, P., Meyerson, B.A., Kihlström, L., Lindquist, C., 1999. Lesion topography and outcome after thermocapsulotomy or gamma knife capsulotomy for obsessive-compulsive disorder: relevance of the right hemisphere. Neurosurgery 44 (3), 452–460.

Luyten, L., Hendrickx, S., Raymaekers, S., Gabriëls, L., Nuttin, B., 2016 Sep. Electrical stimulation in the bed nucleus of the stria terminalis alleviates severe obsessive-compulsive disorder. Mol. Psychiatr. 21 (9), 1272–1280.

Lv, Q., Lv, Q., Yin, D., Zhang, C., Sun, B., Voon, V., et al., 2021 Jan. Neuroanatomical substrates and predictors of response to capsulotomy in intractable obsessive-compulsive disorder. Biol. Psychiatry Cogn. Neurosci. Neuroimaging 6 (1), 29–38.

Lv, Q., Lv, Q., Yin, D., Zhang, C., Sun, B., Voon, V., et al., 2021 Jan. Neuroanatomical substrates and predictors of response to capsulotomy in intractable obsessive-compulsive disorder. Biol. Psychiatry Cogn. Neurosci. Neuroimaging 6 (1), 29–38.

Maldjian, J.A., Laurienti, P.J., Kraft, R.A., Burdette, J.H., 2003 Jul. An automated method for neuroanatomic and cytoarchitectonic atlas-based interrogation of fMRI data sets. Neuroimage 19 (3), 1233–1239.

Mallet, L., Polosan, M., Jaafari, N., Baup, N., Welter, M.-L., Fontaine, D., et al., 2008 Nov. Subthalamic nucleus stimulation in severe obsessive-compulsive disorder. N. Engl. J. Med. 359 (20), 2121–2134.

McCarthy, P., 2021 Apr. FSLeyes. https://doi.org/10.5281/ZENODO.4704476.

Mosley, P.E., Windels, F., Morris, J., Coyne, T., Marsh, R., Giorni, A., et al., 2021 Jun. A randomised, double-blind, sham-controlled trial of deep brain stimulation of the bed nucleus of the stria terminalis for treatment-resistant obsessive-compulsive disorder. Transl. Psychiatry 11 (1). https://doi.org/10.1038/S41398-021-01307-9.

Nanda, P., Banks, G.P., Pathak, Y.J., Sheth, S.A., 2017 Dec. Connectivity-based parcellation of the anterior limb of the internal capsule. Hum. Brain Mapp. 38 (12), 6107–6117.

Nuttin, B., Cosyns, P., Demeulemeester, H., Gybels, J., Meyerson, B., 1999 Oct. Electrical stimulation in anterior limbs of internal capsules in patients with obsessive-compulsive disorder. Lancet (London, England) 354, 1526, 9189.

Pérez-Vigil, A., Mittendorfer-Rutz, E., Helgesson, M., Fernández De La Cruz, L., Mataix-Cols, D., 2019 Apr. Labour market marginalisation in obsessive-compulsive disorder: a nationwide register-based sibling control study. Psychol. Med. 49 (6), 1015–1024.

Peker, S., Samanci, M.Y., Yilmaz, M., Sengoz, M., Ulku, N., Ogel, K., 2020 Sep. Efficacy and safety of gamma ventral capsulotomy for treatment-resistant obsessive-compulsive disorder: a single-center experience. World Neurosurg. 141, e941–e952.

Pustina, D., Avants, B., Faseyitan, O.K., Medaglia, J.D., Coslett, H.B., 2018 Jul. Improved accuracy of lesion to symptom mapping with multivariate sparse canonical correlations. Neuropsychologia 115, 154–166.

Rück, C., Karlsson, A., Steele, J.D., Edman, G., Meyerson, B.A., Ericson, K., et al., 2008 Aug. Capsulotomy for obsessive-compulsive disorder: long-term follow-up of 25 patients. Arch. Gen. Psychiatr. 65 (8), 914–922.

Safadi, Z., Grisot, G., Jbabdi, S., Behrens, T.E., Heilbronner, S.R., McLaughlin, N.C.R., et al., 2018 Feb. Functional segmentation of the anterior limb of the internal capsule: linking white matter abnormalities to specific connections. J. Neurosci. 38 (8), 2106–2117.

Satzer, D., Mahavadi, A., Lacy, M., Grant, J.E., Warnke, P., 2021 Oct. Interstitial laser anterior capsulotomy for obsessive–compulsive disorder: lesion size and tractography correlate with outcome. J. Neurol. Neurosurg. Psychiatry jnnp-2021-327730.

Sinha, S., McGovern, R.A., Mikell, C.B., Banks, G.P., Sheth, S.A., 2015 Jun. Ablative limbic system surgery: review and future directions. Curr. Behav. Neurosci. Rep. 2 (2), 49–59.

Smith, A.H., Choi, K.S., Waters, A.C., Aloysi, A., Mayberg, H.S., Kopell, B.H., et al., 2021 Jan. Replicable effects of deep brain stimulation for obsessive-compulsive disorder. Brain Stimul. 14 (1), 1–3.

Treu, S., Strange, B., Oxenford, S., Neumann, W.J., Kühn, A., Li, N., et al., 2020 Oct. Deep brain stimulation: imaging on a group level. Neuroimage 219, 117018.

Treu, S., Gonzalez-Rosa, J.J., Soto-Leon, V., Lozano-Soldevilla, D., Oliviero, A., Lopez-Sosa, F., et al., 2021 Jul. A ventromedial prefrontal dysrhythmia in obsessive-compulsive disorder is attenuated by nucleus accumbens deep brain stimulation. Brain Stimul. 14 (4), 761–770.

van der Vlis, T.A.M.B., Ackermans, L., Mulders, A.E.P., Vrij, C.A., Schruers, K., Temel, Y., et al., 2021 Feb. Ventral capsule/ventral striatum in obsessive-compulsive disorder: toward a unified connectomic target for deep brain stimulation? Neuromodulation 24 (2), 316–323.

Van Essen, D.C., Smith, S.M., Barch, D.M., Behrens, T.E.J., Yacoub, E., Ugurbil, K., 2013 Oct. The WU-Minn Human Connectome Project: an overview. Neuroimage 80, 62–79.

Whiteside, S.P., Port, J.D., Abramowitz, J.S., 2004 Nov. A meta-analysis of functional neuroimaging in obsessive-compulsive disorder. Psychiatr. Res. 132 (1), 69–79.

Yin, D., Zhang, C.C., Lv, Q., Chen, X., Zeljic, K., Gong, H., et al., 2018 Dec. Dissociable frontostriatal connectivity: mechanism and predictor of the clinical efficacy of capsulotomy in obsessive-compulsive disorder. Biol. Psychiatr. 84 (12), 926–936.

Yushkevich, P.A., Piven, J., Hazlett, H.C., Smith, R.G., Ho, S., Gee, J.C., et al., 2006 Jul. User-guided 3D active contour segmentation of anatomical structures: significantly improved efficiency and reliability. Neuroimage 31 (3), 1116–1128.

Zhan, S., Liu, W., Li, D., Pan, S., Pan, Y., Li, Y., et al., 2014 Apr. Long-term follow-up of bilateral anterior capsulotomy in patients with refractory obsessive-compulsive disorder. Clin. Neurol. Neurosurg. 119, 91–95.

Zhang, C., Kim, S.G., Li, J., Zhang, Y., Lv, Q., Zeljic, K., et al., 2021 Jun. Anterior limb of the internal capsule tractography: relationship with capsulotomy outcomes in obsessive-compulsive disorder. J. Neurol. Neurosurg. Psychiatry 92 (6), 637–644.